Mathematical Modelling and Analysis
Volume 29, Issue 1, 77–89, 2024
https://doi.org/10.3846/mma.2024.17745

Two-Grid Virtual Element Discretization of Quasilinear Elliptic Problem

Fengxin Chen[a], Minghui Yang[b] and Zhaojie Zhou[b]

[a] *School of Science, Shandong Jiaotong University*
250357 Jinan, China
[b] *School of Mathematics and Statistics, Shandong Normal University*
250014 Jinan, China
E-mail(*corresp.*): zhouzhaojie@sdnu.edu.cn

Received October 7, 2022; accepted January 12, 2024

Abstract. In this paper a two grid algorithm for quasilinear elliptic problem based on virtual element method (VEM) discretization is proposed. With this new algorithm the solution of a quasilinear elliptic problem on a fine grid is reduced to the solution of a quasilinear elliptic problem on a much coarser grid, and the solution of a linear system on the fine grid. A priori error estimate in H^1 norm is derived. Numerical experiments are carried out to illustrate the theoretical findings.

Keywords: virtual element method, two grid algorithm, a priori error estimate.

AMS Subject Classification: 65N30.

1 Introduction

Our main goal in this paper is to develop a two grid virtual element algorithm for the following quasilinear elliptic equation:

$$\begin{cases} -\nabla(K(u)\nabla u) = f(x), & \text{in } \Omega, \\ u = 0, & \text{on } \Gamma, \end{cases} \tag{1.1}$$

where $\Omega \subset \mathbb{R}^d$ is a bounded polygonal domain with $\Gamma = \partial\Omega$. The function $K(u) : R \longrightarrow [K_*, K^*]$ is a twice differentiable function with $0 < K_* < K^* < \infty$ and bounded derivatives up to second order. Therefore, $K(u)$ is Lipschitz continuous, namely there exists a positive constant L such that

$$|K(u_1) - K(u_2)| \leq L|u_1 - u_2|. \tag{1.2}$$

It is well-known that for sufficiently smooth f, problem (1.1) possesses a unique solution u; see, e.g., Douglas et al. ([12]).

Due to the flexibility of polygonal meshes to approximate domains with high geometrical complexity the study of polygonal methods(e.g., the polygonal finite element method, extended finite element method (XFEM)) for solving partial differential equations forms a hot topic in recent years. Among these methods the virtual element methods have attracted lots of attentions. The virtual methods can be viewed as an extension of classical finite element method to general polygonal meshes. The VEM is inherently capable of handling hanging nodes arising in the polygonal/polyhedral meshes and hence is more suitable for adaptive mesh refinement. In contrast to finite element methods the basis functions in virtual element space are not known in closed form but are solutions to a partial differential equation, which are never needed to solve in the numerical implementation. Indeed, the VEM only requires the knowledge of a polynomial subspace of the local discrete function space to provide stable and accurate numerical methods. This can be achieved by separating the contribution of the polynomial subspace from that of the remaining nonpolynomial virtual subspace through the introduction of suitable projection operators. Correspondingly the discrete bilinear forms in standard VEM are the sum of a singular part maintaining consistency on polynomials and a stabilizing form enforcing coercivity. Since the VEM was originated in [10] lots of literatures were devoted to construct virtual element discrete schemes for linear or nonlinear problems, for example, elliptic problems([1,7]), parabolic problems([15,20]), Stokes and Navier-Stokes problems ([2,11,13]).

The two-grid algorithms based on finite element methods were originally introduced by Xu [17,18] for the nonsymmetric linear and nonlinear elliptic problems. In these algorithms, two spaces V_h and V_H are employed for the finite element discretization, with mesh size $h \ll H$. The idea of these algorithms is to first solve the original nonsymmetric linear and nonlinear elliptic problems on the coarser finite element space V_H, and then find the solution u_h of a linearized elliptic problem on the finer finite element space V_h based on the coarser level solution u_H. Later on, the two-grid methods were further investigated by many authors, for instance, Xu and Zhou [19] for eigenvalue problems, Bi et al. [3,4,8] for the finite volume element method and the discontinuous Galerkin finite element method for the nonlinear elliptic problems, Wu and Chen et al. [9,16] for the mixed finite element method and [5] for mixed (Navier-)Stokes-Darcy model. The two-grid methods have been shown to be efficient techniques for solving nonlinear problems of various types.

In [6] the authors investigated virtual element approximation of second order quasilinear elliptic problem, and proved the well posedness of the discrete problem and optimal order a priori error estimates. In the present paper we focus on developing a two grid virtual element algorithm for second order quasilinear elliptic problem and deriving a priori error analysis. To the best of our knowledge there are no literatures devoted to develop two grid virtual element algorithm for second order quasilinear elliptic problem. With the help of L^2 projection operators $\Pi_k^{0,h}$ and $\Pi_k^{0,H}$ on different mesh partition $\mathcal{T}_h$ and $\mathcal{T}_H$ we build up a two grid virtual element algorithm for second order quasilinear elliptic problem. With this new algorithm the solution of a quasilinear elliptic problem on a fine grid is reduced to the solution of a quasilinear elliptic problem on a much coarser grid, and the solution of a linear algebraic system on the fine grid. This will improve computational efficiency while ensuring the accuracy, which is verified by numerical experiments.

The paper is organized as follows. In next section, we give some preliminary knowledge about VEM and the discrete scheme for (1.1). In Section 3, a two grid discrete scheme is proposed and a priori error estimate in H^1 norm is proved. In Section 4, numerical example is carried out to verify our theoretical analysis.

2 Virtual element approximation

2.1 Preliminaries

Let $\mathcal{T}_h$ be a family of decompositions of the domain Ω into star-shaped polygonals E and h_E denote the diameter of element E, i.e., the maximum distance between any two points on element E and $h = \sup_{E\in\mathcal{T}_h} h_E$. ∂E denotes the edges of $E \in \mathcal{T}_h$. We make the following assumptions about the regularity of the grid([10]).

- Every element E is star-shaped with respect to every point of a disk D_ρ of radius ρh_E;
- Every edge s of E has length $h_s \geq \rho h_E$;

The virtual element space ([7]) is defined by

$$V_h := \{v_h \in H_0^1(\Omega) : v_h|_E \in V_h^E, \forall E \in \mathcal{T}_h\},$$

where

$$V_h^E := \Big\{v_h \in H^1(E) \cap C^0(\partial E) : \Delta v_h \in \mathbb{P}_k(E), v_h|_s \in \mathbb{P}_k(s)\ \forall\ s \subset \partial E,$$
$$(v_h, p)_{0,E} = (\Pi_{k,E}^{\nabla} v_h, p)_{0,E},\ \forall\ p \in \mathbb{P}_k(E)/\mathbb{P}_{k-2}(E)\Big\}$$

and $\Pi_{k,E}^{\nabla}$ is a projected operator defined as follows.

Definition 1. (See [10]) The projection operator $\Pi_{k,E}^{\nabla} : H^1(E) \to \mathbb{P}_k(E)$ is defined as follows:

$$\begin{cases} (\nabla(\Pi_{k,E}^{\nabla} v_h - v_h), \nabla p)_{0,E} = 0, \forall v_h \in H^1(E), p \in \mathbb{P}_k(E), \\ \displaystyle\int_{\partial E} (v_h - \Pi_{k,E}^{\nabla} v_h) ds = 0,\ \text{if}\ \ k = 1, \\ \displaystyle\int_{E} (v_h - \Pi_{k,E}^{\nabla} v_h) ds = 0,\ \text{if}\ \ k \geq 2. \end{cases}$$

Obviously, we have $\Pi_{k,E}^{\nabla} p = p,\ \forall p \in \mathbb{P}_k(E)$.

DEFINITION 2. (See [7]) The L^2 projection operator $\Pi^0_{k,E} : L^2(E) \to \mathbb{P}_k(E)$ is defined by

$$(\Pi^0_{k,E} v_h - v_h, p)_{0,E} = 0, \forall v_h \in L^2(E), p \in \mathbb{P}_k(E).$$

With slight abuse of notation the symbol Π^0_k will also be used to denote the global operator obtained from the piecewise projections. For the error analysis we also need the following lemmas.

Lemma 1. *(See [7]) There exists a positive constant C such that, for all $E \in \mathcal{T}_h$ and all smooth enough functions $w \in H^s(E)$ defined on E, it holds:*

$$\|w - \Pi^0_{k,E} w\|_{m,E} \le C h_E^{s-m} |w|_{s,E}, \ m = 0, 1, \ 1 \le s \le k+1.$$

Lemma 2. *(See [7])Let $u \in H^1_0(\Omega) \cap H^{s+1}(\Omega)$ with $1 \le s \le k$. Under the assumption on the decomposition $\mathcal{T}_h$, there exist a $u_I \in V_h$ such that*

$$\|u - u_I\| + h|u - u_I|_1 \le C h^{s+1} |u|_{s+1},$$

where C is a positive constant which only depends on the polynomials degree k and mesh regularity.

Lemma 3. *(See [7]) (Approximation using polynomials) Suppose that the assumption on the decomposition $\mathcal{T}_h$ is satisfied and let s be a positive integer such that $1 \le s \le k+1$. Then for any $w \in H^s(E)$ there exists a polynomial $w_\pi \in P^k(E)$ such that*

$$\|w - w_\pi\|_{0,E} + h_E \|w - w_\pi\|_{1,E} \le C h_E^s |w|_{s,E}.$$

2.2 Virtual element discrete scheme

The weak form of (1.1) is defined as follows

$$a(u; u, v) = (f, v), \quad \forall v \in H^1_0(\Omega).$$

Here

$$a(u; u, v) = \int_\Omega K(u) \nabla u \cdot \nabla v dx, \quad \forall u, v \in H^1_0(\Omega).$$

The corresponding virtual element discrete scheme of (1.1) is defined by

$$a_h(u_h; u_h, v_h) = (f, \Pi^0_{k-1} v_h), \quad \forall v_h \in V_h. \tag{2.1}$$

Here

$$a_h(u_h; u_h, v_h) := \sum_{E \in \mathcal{T}_h} a_h^E(u_h; u_h, v_h), \ (f, \Pi^0_{k-1} v_h) := \sum_{E \in \mathcal{T}_h} (f, \Pi^0_{k-1,E} v_h)_{0,E}.$$

The bilinear form a_h^E is any bilinear form on V_h defined as the sum of element-wise contributions a_h^E satisfying the following polynomial consistency property and the stability property.

Assumption: For every $E \in \mathcal{T}_h$ the form a_h^E is bilinear and symmetric in its second and third arguments and satisfies the following properties:

- Polynomial consistency: For all $p \in \mathbb{P}_k(E)$ and for all $v_h \in V_h^E$,

$$a_h^E(z;p,v_h) = \int_E K(\Pi_{k,E}^0 z)\nabla p \cdot \Pi_{k-1,E}^0 \nabla v_h dx, \forall z \in L^2(E). \tag{2.2}$$

- Stability: There exist positive constants α_* and α^* independent of h and the mesh element E such that

$$\alpha_* a^E(z_h;v_h,v_h) \leq a_h^E(z_h;v_h,v_h) \leq \alpha^* a^E(z_h;v_h,v_h),\ \forall z_h, v_h \in V_h^E. \tag{2.3}$$

Remark 1. We remark that the following error analysis is valid whenever the assumption above is satisfied. In the numerical tests a particular choice of local bilinear forms([6]) is given below:

$$a_h(u_h;u_h,v_h) := \sum_{E\in\mathcal{T}_h} a_h^E(u_h;u_h,v_h) = \sum_{E\in\mathcal{T}_h} \Big(\int_E K(\Pi_{k,E}^0 u_h)$$
$$\times \Pi_{k-1,E}^0 \nabla u_h \cdot \Pi_{k-1,E}^0 \nabla v_h dx + S^E(u_h; u_h - \Pi_{k,E}^0 u_h, v_h - \Pi_{k,E}^0 v_h)\Big).$$

Here

$$S^E(u_h; u_h - \Pi_{k,E}^0 u_h, v_h - \Pi_{k,E}^0 v_h)$$
$$:= K_E(\Pi_{0,E}^0 u_h) h_E^{d-2} \sum_{r=1}^{N^E} \mathrm{dof}_r(u_h - \Pi_{k,E}^0 u_h)\mathrm{dof}_r(v_h - \Pi_{k,E}^0 v_h),$$

where N^E is the number of degrees of freedom on the element E and $\mathrm{dof}_r(u_h - \Pi_k^0 u_h)$ denotes the value of the rth local degree of freedom defining $u_h - \Pi_k^0 u_h$ in V_h^E.

According to [6] we have the existence of a solution u_h of (2.1).

Lemma 4. *Let $f \in L^2(\Omega)$ be given and assume that (1.2) holds. Choose $M > 0$ such that $\|f\| \leq MK_*\alpha_*$. Then there exists a solution $u_h \in \mathcal{B} = \{v_h \in V_h; \|\nabla v_h\| \leq M\}$ of (2.1).*

Moreover, according to [6] the following error estimates hold.

Lemma 5. *Suppose that u is the solution of (1.1) and $u \in H^s(\Omega) \cap W^{1,\infty}(\Omega)$, $s \geq 2$. Assuming that $f \in H^{s-1}(\Omega)$ and $K(u) \in W^{s-1,\infty}(\Omega)$, with Ω convex. Let $u_h \in V_h$ be the solution of (2.1). Then there exists a constant C independent of h such that, for h sufficiently small,*

$$\|u - u_h\| + h\|\nabla(u - u_h)\| \leq Ch^r, \ \ r = \min(s, k+1).$$

3 Two grid virtual element discrete scheme and error analysis

In this section, we present a two-grid virtual element algorithm for the quasilinear elliptic problem and derive the corresponding error estimate.

Let $\mathcal{T}_h$ and $\mathcal{T}_H$ be two mesh partition with elements $E, \widetilde{E}$ and mesh parameter $h, H (h \ll H)$, respectively. The corresponding virtual element spaces are associated with V_h and V_H. For the sake of clarity we denote by $\Pi_k^{0,h}$ and $\Pi_k^{0,H}$ the L^2 projection with different mesh partition $\mathcal{T}_h$ and $\mathcal{T}_H$. Then the two grid virtual element algorithm for (1.1) is defined as follows:

- **Step 1: Solving the following nonlinear problem on a coarse grid**

$$a_H(u_H; u_H, v_H) = (f, \Pi_{k-1}^{0,H} v_H), \quad \forall v_H \in V_H. \tag{3.1}$$

- **Step 2: Solving the following linear problem on a fine grid**

$$\widetilde{a}_h(u_H; U_h, v_h) = (f, \Pi_{k-1}^{0,h} v_h), \quad \forall v_h \in V_h. \tag{3.2}$$

Here $\widetilde{a}_h(u_H; U_h, v_h) := \sum_{E \in \mathcal{T}_h} a_h^E(u_H; U_h, v_h)$. In the bilinear form $a_h^E(u_H; U_h, v_h)$ the coefficient in each element takes the form $K((\Pi_k^{0,H} u_H)|_E)$.

In above algorithm we utilize the virtual element method to solve the quasilinear elliptic problem on a coarse space V_H, and obtain a rough approximation $u_H \in V_H$. Then we use it to linearize the corresponding system on the fine space V_h, and solve the resulting linearized problem to obtain $U_h \in V_h$. Since the dim(V_H)$\leq$ dim(V_h), the computational cost for u_H is relatively small. This implies that the work for solving the quasilinear problem is not much difficult than solving a linear problem.

Theorem 1. *Let U_h be the solution of the two grid virtual element discrete scheme (3.1)–(3.2). Then under the assumption of Lemma 5 we can derive*

$$\|u - U_h\|_1 \leq C(h^{r-1} + H^r), \ \ r = \min(s, k+1).$$

Proof. Let $u_I \in V_h$, $\psi = U_h - u_I$. Set $c_* := K_* \alpha_*$. By (2.1), (3.2) we derive

$$\begin{aligned} c_* \|U_h - u_I\|_1^2 &\leq \widetilde{a}_h(u_H; U_h - u_I, U_h - u_I) = \widetilde{a}_h(u_H; U_h, \psi) - \widetilde{a}_h(u_H; u_I, \psi) \\ &= (\Pi_{k-1}^{0,h} f, \psi) - \widetilde{a}_h(u_H; u_I, \psi) = (\Pi_{k-1}^{0,h} f - f, \psi) + a(u; u, \psi) - \widetilde{a}_h(u_H; u_I, \psi) \\ &= (\Pi_{k-1}^{0,h} f - f, \psi) + a(u; u, \psi) - \sum_{E \in \mathcal{T}_h} a_h^E(u_H; u_\pi, \psi) - \sum_{E \in \mathcal{T}_h} a_h^E(u_H; u_I - u_\pi, \psi), \end{aligned}$$

where $u_\pi \in \mathbb{P}_k(E)$ is the polynomial approximation of u given by Lemma 3. Then, using the polynomial consistency leads to

$$\begin{aligned} c_* \|U_h - u_I\|_1^2 &\leq (\Pi_{k-1}^{0,h} f - f, \psi) - \sum_{E \in \mathcal{T}_h} a_h^E(u_H; u_I - u_\pi, \psi) \\ &+ \sum_{E \in \mathcal{T}_h} \int_E (K(u) - K((\Pi_k^{0,H} u_H)|_E)) \nabla u \cdot \nabla \psi dx + \sum_{E \in \mathcal{T}_h} \int_E K((\Pi_k^{0,H} u_H)|_E) \nabla u \end{aligned}$$

$$
\begin{aligned}
&\cdot \nabla\psi dx - \sum_{E\in\mathcal{T}_h}\int_E K((\Pi_k^{0,H}u_H)|_E)\nabla u_\pi \cdot \Pi_{k-1,E}^{0,h}\nabla\psi dx = (\Pi_{k-1}^{0,h}f - f, \psi) \\
&- \sum_{E\in\mathcal{T}_h} a_h^E(u_H; u_I - u_\pi, \psi) + \sum_{E\in\mathcal{T}_h}\int_E (K(u) - K((\Pi_k^{0,H}u_H)|_E))\nabla u \cdot \nabla\psi dx \\
&\quad + \sum_{E\in\mathcal{T}_h}\int_E K((\Pi_k^{0,H}u_H)|_E)\nabla(u-u_\pi)\cdot\nabla\psi dx \\
&\quad + \sum_{E\in\mathcal{T}_h}\int_E K((\Pi_k^{0,H}u_H)|_E)\nabla u_\pi \cdot (\nabla\psi - \Pi_{k-1,E}^{0,h}\nabla\psi)dx := \sum_{i=1}^{5} T_i. \qquad (3.3)
\end{aligned}
$$

Next, we will bound the various terms $T_i, i = 1, \ldots, 5$. Using Lemma 1 we have

$$T_1 = (\Pi_{k-1}^{0,h}f - f, \psi - \Pi_0^{0,h}\psi) \le Ch^{r-1}\|f\|_{r-2}\|\nabla\psi\|.$$

Nextly, we easily obtain

$$T_2 \le C(\|u-u_\pi\|_1 + \|u-u_I\|_1)\|\nabla\psi\| \le Ch^{r-1}\|u\|_r\|\nabla\psi\|.$$

Using the fact that $K(u)$ is Lipsitchz continuous and the stability of $\Pi_k^{0,H}$ in L^2 norm leads to

$$T_3 \le C(\|u - \Pi_k^{0,H}u\| + \|u-u_H\|)\|\nabla u\|_{L^\infty}\|\nabla\psi\| \le CH^r\|\nabla\psi\|.$$

Also, using the fact that $K(u)$ is bounded along with Theorem 3.2, we obtain

$$T_4 \le C\|u-u_\pi\|_1\|\nabla\psi\| \le Ch^{r-1}\|u\|_r\|\nabla\psi\|.$$

Finally, we can rearrange the last term as follows

$$
\begin{aligned}
&\sum_{E\in\mathcal{T}_h}\int_E K((\Pi_k^{0,H}u_H)|_E)\nabla u_\pi\cdot(\nabla\psi - \Pi_{k-1,E}^{0,h}\nabla\psi)dx \\
&\quad = \sum_{E\in\mathcal{T}_h}\int_E K((\Pi_k^{0,H}u_H)|_E)\nabla(u_\pi - u)\cdot(I - \Pi_{k-1,E}^{0,h})\nabla\psi dx \\
&\quad + \sum_{E\in\mathcal{T}_h}\int_E K((\Pi_k^{0,H}u_H)|_E)\nabla u\cdot(I - \Pi_{k-1,E}^{0,h})\nabla\psi dx \\
&= \sum_{E\in\mathcal{T}_h}\int_E K((\Pi_k^{0,H}u_H)|_E)\nabla(u_\pi - u)\cdot(I - \Pi_{k-1,E}^{0,h})\nabla\psi dx \\
&\quad + \sum_{E\in\mathcal{T}_h}\int_E (K((\Pi_k^{0,H}u_H)|_E) - K(u))\nabla u\cdot(I - \Pi_{k-1,E}^{0,h})\nabla\psi dx \\
&\quad + \sum_{E\in\mathcal{T}_h}\int_E (K(u)\nabla u)\cdot(I - \Pi_{k-1,E}^{0,h})\nabla\psi dx
\end{aligned}
$$

$$
\begin{aligned}
&= \sum_{E\in\mathcal{T}_h}\int_E K((\Pi_k^{0,H}u_H)|_E)\nabla(u_\pi - u)\cdot(I-\Pi_{k-1,E}^{0,h})\nabla\psi dx \\
&\quad + \sum_{E\in\mathcal{T}_h}\int_E (K((\Pi_k^{0,H}u_H)|_E)-K(u))\nabla u\cdot(I-\Pi_{k-1,E}^{0,h})\nabla\psi dx \\
&\quad\quad + \sum_{E\in\mathcal{T}_h}\int_E (I-\Pi_{k-1,E}^{0,h})(K(u)\nabla u)\cdot\nabla\psi dx := S_1+S_2+S_3.
\end{aligned}
$$

In view of the stability of $\Pi_{k-1}^{0,h}$ and the boundedness of $K(u)$ we deduce

$$S_1 \le C\|\nabla(u_\pi - u)\|\|\nabla\psi\| \le Ch^{r-1}\|u\|_r\|\nabla\psi\|.$$

By the fact that $K(u)$ is Lipsitchz continuous and the stability of $\Pi_k^{0,H}$ we have

$$S_2 \le C(\|u-\Pi_k^{0,H}u\| + \|u-u_H\|)\|\nabla u\|_{L^\infty}\|\nabla\psi\| \le CH^r\|u\|_r\|\nabla\psi\|.$$

For S_3 we have

$$S_3 \le C\|(I-\Pi_{k-1}^{0,h})(K(u)\nabla u)\|)\|\nabla\psi\| \le Ch^{r-1}\|u\|_r\|\nabla\psi\|.$$

Collecting above estimates yields

$$T_5 \le C(h^{r-1}+H^r)\|\nabla\psi\|.$$

Inserting the estimates of $T_1 \backsim T_5$ into (3.3) leads to the following result

$$\|U_h - u_I\|_1 \quad\le\quad Ch^{r-1}+CH^r.$$

Then we obtain

$$\|u-U_h\|_1 \le \|u-u_I\|_1 + \|u_I - U_h\|_1 \le Ch^{r-1}+CH^r.$$

□

4 Numerical experiments

In this section, we will verify the theoretical analysis by numerical experiment using the two-grid algorithm. Numerical experiment is carried out on an Intel Xeon-6138 CPU. The square mesh, lloyd mesh (see [14]) and non-convex polygon mesh are used, which are shown in Figure 1, respectively. Since the basis functions are unknown inside the elements, the H^1 errors are computing using the local projector Π_k^0 by the following way:

$$H^1 \text{ norm error: } e_{h,1} = \sqrt{\sum_{E\in\mathcal{T}_h} |u-\Pi_k^0 U_h|^2_{H^1(E)}},$$

where u is the exact solution and U_h is the numerical solution. In the first step of two-grid algorithm, the fixed-point iterative method is employed to solve quasilinear discretization equation. The finer mesh is generated by the software PolyMesher([14]).

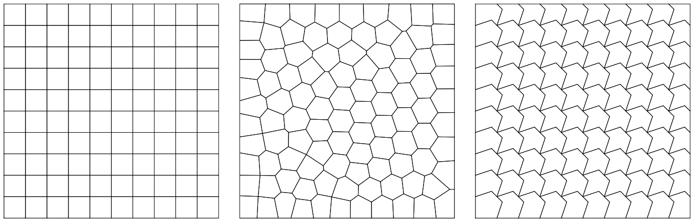

Figure 1. Three meshes:(a) square, (b) lloyd, (c) non-convex.

Example 1. Consider the following test problem on the unit square $\Omega = [0,1] \times [0,1]$ proposed by [3] with the exact solution

$$u(x,y) = \sin(3\pi x)\sin(3\pi y), \quad K(u) = 1 + 1/(1+u^2).$$

The source function f is determined by u and $K(u)$. We report the numerical results of two-grid algorithm with $k = 1$ on different meshes. Moreover, Theorem 3.1 suggests that the optimal rate of convergence in the two-grid method can be achieved by employing $H = O(\sqrt{h})$. Therefore, in the numerical experiments we set $H = O(\sqrt{h})$. The calculation formula of convergence order is as follows:

$$Rate = \log(e_{h_i,1}/e_{h_j,1})/\log(h_i/h_j),$$

where e_{h_i}, e_{h_j} represent the errors on the same type of grid with maximum diameter h_i, h_j respectively.

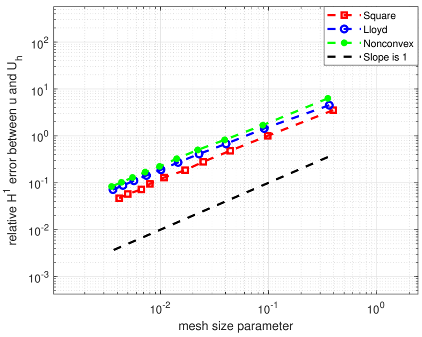

Figure 2. The convergence curves of $e_{h,1}$ on three meshes.

The H^1 error $e_{h,1}$ and convergence order of some numerical results are reported in Tables 1–3 for a set of combination of h and H on square, lloyd and non-convex polygon meshes. The convergence curves of $e_{h,1}$ on three meshes are shown in Figure 2. We can observe that the convergence curves are parallel to the line with slope 2. This implies that the two grid algorithm developed in Section 3 have the optimal convergence rate for different meshes.

Table 1. Error table for Example 1 on square meshes.

H	h	$e_{h,1}$	Rate$_H$	Rate$_h$
0.1768	0.0221	5.0114e-1	\	\
0.1414	0.0141	3.2647e-1	2.0801	0.9602
0.1010	0.0072	1.6901e-1	1.9567	0.9783
0.0884	0.0055	1.2981e-1	1.9767	0.9884
0.0786	0.0044	1.0254e-1	2.0013	1.0006

Table 2. Error table for Example 1 on lloyd meshes.

H	h	$e_{h,1}$	Rate$_H$	Rate$_h$
0.3548	0.0983	1.6721e0	\	\
0.1899	0.0249	4.6645e-1	2.0420	0.9292
0.1555	0.0169	3.0917e-1	2.0609	1.0703
0.0954	0.0067	1.2036e-1	1.9309	1.0119
0.0776	0.0042	7.8033e-2	2.1019	0.9190
0.0688	0.0033	6.1338e-2	2.0065	1.0021

Table 3. Error table for Example 1 on non-convex meshes.

H	h	$e_{h,1}$	Rate$_H$	Rate$_h$
0.1822	0.0228	5.1466e-1	\	\
0.1458	0.0146	3.3951e-1	1.8642	0.9321
0.0911	0.0057	1.3813e-1	1.9134	0.9567
0.0810	0.0045	1.0971e-1	1.9557	0.9779
0.0729	0.0036	8.9380e-2	1.9453	0.9727

Table 4. Comparison between two-grid algorithm and fixed-point iterative method for Example 1.

Mesh	H	h	parameter	Two-grid algor.	Fixed-point iter.
square	0.1414	0.0141	$e_{h,1}$	3.2647e-1	2.5649e-1
			time	19.0560s	76.8149s
lloyd	0.1555	0.0169	$e_{h,1}$	3.0917e-1	2.5405e-1
			time	21.6075s	92.5125s
non-convex	0.1458	0.0146	$e_{h,1}$	3.3951e-1	2.6454e-1
			time	23.1257s	110.6263s

In Tables 4–5, we report the comparison results of the two-grid algorithm and fixed-point iterative method for solving the above quasilinear problems on

Table 5. Comparison between two-grid algorithm and fixed-point iterative method for Example 1.

Mesh	H	h	parameter	Two-grid algor.	Fixed-point iter.
square	0.1010	0.0072	$e_{h,1}$ time	1.6901e-1 72.3592s	1.3083e-1 316.6477 s
lloyd	0.1047	0.0079	$e_{h,1}$ time	1.5601e-1 99.4753s	1.2707e-1 428.3219s
non-convex	0.1041	0.0074	$e_{h,1}$ time	1.7887e-1 83.4171s	1.3489e-1 381.8415s

Table 6. Error table for Example 1 on square meshes with $k = 2$.

H	h	$e_{h,1}$	Rate$_H$	Rate$_h$
0.4714	0.3536	2.9375e0	\	\
0.2828	0.1571	6.6891e-1	2.8967	1.8247
0.2357	0.1179	3.7815e-1	3.1282	1.9825
0.1767	0.0744	1.5209e-1	3.1661	1.9821
0.1285	0.0456	5.7421e-2	3.0587	1.9897

Table 7. Error table for Example 1 on lloyd meshes with $k = 2$.

H	h	$e_{h,1}$	Rate$_H$	Rate$_h$
0.3970	0.2507	1.2534e-0	\	\
0.2987	0.1647	5.5831e-1	2.8409	1.9259
0.2159	0.0990	2.0803e-1	3.0445	1.9382
0.1503	0.0586	6.5421e-2	3.1962	2.1075
0.1387	0.0517	5.1083e-2	3.0587	1.9901

different meshes. Two-grid algorithm is performed on a set of combination of h and H as shown in Tables 4–5, and the fixed-point iteration method is performed with mesh size h. From the data, we find that the H^1 errors of them are almost the same, but the time of the two-grid algorithm is much less than that of the fixed-point iterative method. Therefore, it can be seen that the two-grid algorithm can save a lot of computing time while maintaining the accuracy.

We also carry out numerical experiment on the virtual element space with $k = 2$ for square and lloyd polygon meshes. The errors and convergence rates are presented in Tables 6–7. The Theorem 1 suggests that optimal rate of convergence in the two-grid method using quadratic virtual element space ($k = 2$) can be achieved by employing $H = O(h^{2/3})$. From Tables 6–7 we can observe that the convergence rates are optimal.

Acknowledgements

The research was supported by Natural Science Foundation of Shandong Province (No. 2016JL01004).

References

[1] D. Adak, S. Natarajan and E. Natarajan. Virtual element method for semilinear elliptic problems on polygonal meshes. *Applied Numerical Mathematics*, **145**:175–187, 2019. https://doi.org/10.1016/j.apnum.2019.05.021.

[2] P.F. Antonietti, L. Beirão da Veiga, D. Mora and M. Verani. A stream virtual element formulation of the Stokes problem on polygonal meshes. *SIAM Journal on Numerical Analysis*, **52**(1):386–404, 2014. https://doi.org/10.1137/13091141X.

[3] C. Bi and V. Ginting. Two-grid finite volume element method for linear and nonlinear elliptic problems. *Numerische Mathematik*, **108**:177–198, 2007. https://doi.org/10.1007/s00211-007-0115-9.

[4] C. Bi and V. Ginting. Two-grid discontinuous galerkin method for quasilinear elliptic problems. *Journal of Scientific Computing*, **49**:311–331, 2011. https://doi.org/10.1007/s10915-011-9463-9.

[5] M. Cai, M. Mu and J. Xu. Numerical solution to a mixed Navier–Stokes/Darcy model by the two-grid approach. *SIAM Journal on Numerical Analysis*, **47**(5):3325–3338, 2009. https://doi.org/10.1137/080721868.

[6] A. Cangiani, P. Chatzipantelidis, G. Diwan and E.H. Georgoulis. Virtual element method for quasilinear elliptic problems. *IMA Journal of Numerical Analysis*, **40**(4):2450–2472, 2020. https://doi.org/10.1093/imanum/drz035.

[7] A. Cangiani, G. Manzini and O.J. Sutton. Conforming and nonconforming virtual element methods for elliptic problems. *IMA Journal of Numerical Analysis*, **37**(3):1317–1354, 2016. https://doi.org/10.1093/imanum/drw036.

[8] C. Chen, M. Yang and C. Bi. Two-grid methods for finite volume element approximations of nonlinear parabolic equations. *Journal of Computational and Applied Mathematics*, **228**(1):123–132, 2009. https://doi.org/10.1016/j.cam.2008.09.001.

[9] L. Chen and Y. Chen. Two-grid method for nonlinear reaction-diffusion equations by mixed finite element methods. *Journal of Scientific Computing*, **49**(3):383–401, 2011. https://doi.org/10.1007/s10915-011-9469-3.

[10] L. Beirão da Veiga, F. Brezzi, A. Cangiani, G. Manzini, L.D. Marini and A. Russo. Basic principles of virtual element methods. *Mathematical Models and Methods in Applied Sciences*, **23**(01):199–214, 2013. https://doi.org/10.1142/S0218202512500492.

[11] L. Beirão da Veiga, C. Lovadina and G. Vacca. Virtual elements for the Navier-Stokes problem on polygonal meshes. *SIAM Journal on Numerical Analysis*, **56**(3):1210–1242, 2018. https://doi.org/10.1137/17M1132811.

[12] J. Douglas Jr, T. Dupont and J. Serrin. Uniqueness and comparison theorems for nonlinear elliptic equations in divergence form. *Archive for Rational Mechanics and Analysis*, **42**(3):157–168, 1971. https://doi.org/10.1007/BF00250482.

[13] X. Liu, J. Li and Z. Chen. A nonconforming virtual element method for the Stokes problem on general meshes. *Computer Methods in Applied Mechanics and Engineering*, **320**:694–711, 2017. https://doi.org/10.1016/j.cma.2017.03.027.

[14] C. Talischi, G.H. Paulino, A. Pereira and I.F.M. Menezes. Polymesher: a general-purpose mesh generator for polygonal elements written in Matlab. *Structural and Multidisciplinary Optimization*, **45**:309–328, 2012. https://doi.org/10.1007/s00158-011-0706-z.

[15] G. Vacca and L. Beirão da Veiga. Virtual element methods for parabolic problems on polygonal meshes. *Numerical Methods for Partial Differential Equations*, **31**(6):2110–2134, 2015. https://doi.org/10.1002/num.21982.

[16] L. Wu and M.B. Allen. A two-grid method for mixed finite-element solution of reaction-diffusion equations. *Numerical Methods for Partial Differential Equations*, **15**(3):317–332, 1999. https://doi.org/10.1002/(SICI)1098-2426(199905)15:3¡317::AID-NUM4¿3.0.CO;2-U.

[17] J. Xu. A novel two-grid method for semilinear elliptic equations. *SIAM Journal on Scientific Computing*, **15**(1):231–237, 1994. https://doi.org/10.1137/0915016.

[18] J. Xu. Two-grid discretization techniques for linear and nonlinear PDEs. *SIAM Journal on Numerical Analysis*, **33**(5):1759–1777, 1996. https://doi.org/10.1137/S0036142992232949.

[19] J. Xu and A. Zhou. A two-grid discretization scheme for eigenvalue problems. *Mathematics of Computation*, **70**(233):17–25, 2001. https://doi.org/10.1090/S0025-5718-99-01180-1.

[20] J. Zhao, B. Zhang and X. Zhu. The nonconforming virtual element method for parabolic problems. *Applied Numerical Mathematics*, **143**:97–111, 2019. https://doi.org/10.1016/j.apnum.2019.04.002.